Journal of Polyphenols
2025, 7 (1): 20–31
journal homepage: http://jpolyph.syphu.edu.cn

Network pharmacology and molecular docking based study on the potential mechanism of the treatment of colitis by *Solanum nigrum* Linn.

Bingxin Zhang, Zhennan Meng, Kexin Huang, Ziqi Sun, Xiaoshu Zhang *

Faculty of Functional Food and Wine, Shenyang Pharmaceutical University, Shenyang 110016, China

Abstract The purpose of this study was to characterize the chemical components of the extract of *Solanum Nigrum* Linn. (SNL), by LC-MS/MS, and to identify 33 compounds by positive and negative total ion flow maps. Network pharmacology and molecular docking methods were used to investigate the mechanism of action of SNL against ulcerative colitis (UC). A total of 282 component target genes and 1 850 disease target genes were obtained, and 157 cross-targets and 16 core-targets were obtained after crossover. A total of 20 signaling pathways such as anti-inflammatory and anti-apoptotic were obtained by GO analysis and KEGG analysis, respectively. It is possible that the anti UC effect can be achieved by regulating proteins such as AKT1, EGFR, NFKB1, JUN, and HSP90AA1. Molecular docking results show that the anti UC active ingredients are well docked with the target protein molecules This study provides a scientific basis for the development and utilization of SNL.

Keywords: LC-MS/MS; ulcerative colitis; network pharmacology; molecular docking; *Solanum Nigrum* Linn.

1 Introduction

Ulcerative colitis (UC) is an inflammatory bowel disease (IBD) whose pathogenesis is associated with autoimmune abnormalities. The main etiology of UC is the disruption of the intestinal barrier, which leads to an immune imbalance of the intestinal barrier, triggering inflammation and accelerating the progression of the disease [1]. In recent years, a large number of studies have been conducted to develop drugs for the prevention and treatment of UC, starting from natural immunity and using herbal compounds or active ingredients. *Solanum nigrum* Linn. (SNL) is rich in many nutrients, such as polysaccharides, flavonoids, amino acids and polyphenols. At the same time, SNL is a kind of medicine and food fruit, with anti-tumor, heat detoxification, anti-inflammatory, and other effects [2].

Some studies have shown the anticancer cell effects of SNL polyphenol substance [3]. But nowadays there are relatively few studies with polyphenols from SNL on colitis. The aim of this paper is to further investigate the therapeutic mechanism of polyphenol substances in SNL on UC through LC-MS/MS, network pharmacology and molecular docking.

2 Materials and methods

2.1 Chemicals and reagents

SNL was harvested in September in the suburbs of Shenyang City, Liaoning Province, China.

* Corresponding author: Xiaoshu Zhang (xiaoshu2397@163.com).
These authors have no conflict of interest to declare.

2.2 Extraction of SNL polyphenols

Weigh 20 g of SNL, grind them with a mortar and pestle, add 200 mL of pure water at 100 °C for 50 min of hot extraction, then add 200 mL of anhydrous ethanol and water bath at 50 °C for 2 h, filter the resulting ethanol extract through filter paper, and rotary evaporate and concentrate at 40 °C for 2 h, and naturally air-dry the resulting concentrate.

2.3 Determination of total polyphenols

Total polyphenols in SNL extract was determined by colorimetric method using forintol [4].

2.3.1 Handling of standards

Accurately weigh 0.1 g gallic acid, dissolve with 50 mL of distilled water, and then condense to 100 mL to obtain the gallic acid standard stock solution with mass concentration of 1 000 mg/L. Take 0, 1.25, 2.5, 5, 10, 20, 40 mL of the standard stock solution in a 100 mL volumetric flask, and then condense to the scale with distilled water to prepare a series of standard solutions with mass concentrations of 0, 12.5, 25, 50, 100, 200, and 400 mg/L. The standard solution was then prepared as follows the series standard solutions were prepared with mass concentrations of 0, 12.5, 25, 50, 100, 200 and 400 mg/L.

2.3.2 Treatment of sample

Weigh 0.02 g of sample, add 200 uL of distilled water and dissolve. After centrifugation at 3 000 r/min for 10 min, take its supernatant and dilute 50 times.

2.3.3 Determination and calculation

Take 0.5 mL of standard solution or sample solution in a centrifuge tube, respectively, add 0.5 mL of forintol colorant 1.5 mL of 20% Na_2CO_3, mix well, and react in a water bath at 50 ℃ for 30 min. absorbance was measured at 765 nm. Three parallel tests were done for each concentration, and the average value was taken to make the standard curve, to obtain the regression equation between the absorbance value A and the concentration of gallic acid standard solution (T, mg/L), and the total polyphenol content was calculated according to the following formula.

$$W = \frac{C \times V \times N}{M}$$

W: Total phenol content mg/L; *C*: Gallic acid mass concentration mg/L; *V*: Extract volume/mL; *N*: Dilution; *M*: Sampling volume/g.

2.4 LC-MS/MS analysis

The extracts of SNL were analyzed by full scanning under positive and negative ion modes. Parameters for liquid chromatography: Agilent 1260 HPLC system equipped with Agilent ZORBAX bsC_{18} column, column temperature set at 30 ℃. Agilent 1260 HPLC system equipped with Agilent ZORBAX bsC_{18} column, column temperature set at 30 ℃. The temperature of the automatic sampler was set at 4 ℃, the sample volume was set at 1 μL, and the flow rate was set at 1 mL/min. The mobile phase consisted of 0.1% phosphoric water and methanol. Gradient conditions: 0−5 min, 2% methanol; 5−10 min, 2%−5% methanol; 10−40 min, 5%−45% methanol; 40−60 min, 45% methanol. Parameters used for mass spectrum: Agilent 6530 MS/MS mass spectrometer, positive and negative ion modes using electrospray ionization (ESI). The MS scanning range is set to 100−500 Da, and the MS/MS scanning range is set to 50−500 Da. The capillary voltage was set at 3.5 kV, the dry gas flow was set at 9 mL/min, and the temperature was set at 350 ℃.The atomizer gas pressure is set at 45 psi. Sheath gas flow and temperature were maintained at 12 mL/min and 400 ℃, respectively. Nitrogen is used as an auxiliary gas as well as an atomizing gas.

The fragmentation voltage and collision energy (CE) were set at 150 V and 40 V, respectively. Agilent MassHunter workstation was used for data acquisition (version B.05.01). Data were processed using Agilent MassHunter qualitative analysis (version B.06.00).

2.5 Screening of active ingredients and prediction of action targets

The active ingredients of SNL analyzed by LC-MS were used as the research object, and were searched in the PubChem (https://pubchem.ncbi.nlm.nih.gov/) database, and the corresponding Isomeric SMILES numbers were queried according to the names of the ingredients, and finally the targets were imported into Swiss ADME (http://SwissADME/) database, and the species was limited to "Homo sapiens", and the official gene names of the targets were obtained. Finally, the target was imported into the Swiss Target Prediction (http://swisstargetprediction.ch/) database, and the species was qualified as "Homo sapiens", the official gene name of the target was obtained, and the data was imported into the Excle table, and the "Probability" was set as the initial screening. The data were imported into the Excle table and set "Probability > 0" as the preliminary screening condition; the compound-target network diagram was constructed by using Cytoscape 3.9.1 software.

2.6 Access to relevant targets

Using "ulcer colitis" as the keyword, GeneCards (https://www.genecards.org/) and OMIM (https://www.omim.org/) were used to screen the relevant targets, and the two disease databases were merged to create a Venn diagram using Venny 2.1.0 (https://www.genecards.org/). The target information of the two disease databases was combined, and the Venn diagram was drawn using Veen 2.1.0 (https://bioinfogp.cnb.csic.es/tools/venny/).

2.7 Construction of active ingredient target network and protein interactions network

Disease drug critical genes were obtained by Venn. Cytoscape 3.9.0 software was used to create the active ingredient target network diagram, and with the help of String (https://cn.string-db.org/) database, the species was set as "Homo sapiens", and the default minimum interactions score was 0.4, so as to obtain the protein-protein interaction (PPI) network map was created with the help of String database, and the species was set as "Homo sapiens".

2.8 Gene ontology and KEGG analyse

Common targets were analyzed using the Metascape platform (https://metascape.org/gp/index.html#/main/step1) and visualized using the online mapping platform Microbiology (http://www.bioinformatics.com.cn/).

2.9 Prediction of key active ingredients

Cytoscape 3.9.0 software was used to predict the key active ingredients.

2.10 Molecular docking

According to the "drug-active ingredient-target" network and PPI network diagram, the top 10 core targets and the top 5 key ingredients in terms of degree value were screened out for molecular docking. The 3D structures of the key target proteins were downloaded from the PDB (https://www.rcsb.org/) database, and the 3D structures of the proteins and active ingredients were processed by using AutoDockTools 1.5.7 software to dehydrate, remove the original ligands, hydrogenate, and calculate the binding energies, and then the processed results were visualized.

3 Results

3.1 Calculation of total phenol content

The total polyphenols content was calculated as 12.8 mg/g from the standard curve $y = 0.571\ 5x - 0.735\ 9$.

3.2 LC-MS/MS analysis of SNL extracts

The LC-MS/MS analysis of SNL initially identified 33 compounds, 30 of which were identified by positive ionization mode. There were five phenolic

compounds, ferulic acid, caffeic acid, *p*-coumaric acid, chlorogenic acid, and nicotinic acid. The identification of each compound was finalized on the basis of molecular weight, retention time (t_R), fragmentation ions, chemical class, and name of each compound (Table 1 and Table 2). The LC-MS/MS positive and negative ion chromatograms of SNL are shown in Fig. 1 and Fig. 2.

Table 1 Compounds identified in SDL extract by LC-MS/MS at positive ion mode

No.	t_R (min)	Precursor ion $[M + H]^+$ (m/z)	Theoretical mass (m/z)	Elemental composition	Name of the compound
1	1.491	74.060	74.050	C_3H_7NO	N,N-Dimethylformamide
2	1.491	112.087	112.074	$C_5H_9N_3$	Histamine
3	1.491	117.138	117.086	$C_6H_{16}N_2$	Hexamethylenediamine
4	1.616	266.123	266.107	$C_{10}H_{19}NO_7$	3-Hydroxy-N-[[3,4,5-trihydroxy-6-(hydroxymethyl)oxan-2-yl]methyl] propanamide
5	1.616	118.086	118.052	$C_5H_{11}NO_2$	Valine
6	2.424	230.988	230.844	$C_7H_6N_2O_3S_2$	6-Hydroxy-1,3-benzothiazole-2-sulfonamide
7	2.424	206.100	206.073	$C_{12}H_{15}NS$	5-Phenylpentyl isothiocyanate
8	2.424	314.084	314.044	$C_9H_{11}N_7O_6$	6-Aminooxy-5-[(2-hydroxy-4-methoxy-6-oxo-2,3-dihydro-1H-pyrimidin-5-yl)diazenyl]-1H-pyrimidine-2,4-dione
9	5.436	166.086	166.132	$C_9H_{11}NO_2$	Phenylalanine
10	5.436	177.101	177.046	$C_{10}H_{12}N_2O$	Cotinine
11	35.677	298.096	298.065	$C_{11}H_{15}N_5O_3S$	5’-Deoxy-5’-methylthioadenosine
12	35.677	487.141	487.064	$C_{17}H_{22}N_6O_{11}$	Trinitrophenylglutamyllysine
13	36.594	163.039	163.062	$C_9H_6O_3$	Umbelliferone
14	36.594	377.086	377.133	$C_{18}H_{16}O_9$	Limocitrol
15	37.528	427.208	427.109	$C_{21}H_{26}N_6O_4$	4-Amino-2-(2-methoxyethoxy)-8-[[3-(pyrrolidin-1-ylmethyl)phenyl]methyl]-5H-pteridine-6,7-dione
16	37.987	457.217	457.204	$C_{26}H_{28}N_6S$	4-{3-[2-(7-Methyl-1H-indol-3-yl)-ethylsulfanyl]-5-quinolin-2-yl-[1,2,4]triazol-4-yl}-butylamine
17	38.179	305.157	305.134	$C_{11}H_{16}N_{10}O$	bis[(2S)-2-(2H-tetrazol-5-yl)pyrrolidin-1-yl] methanone
18	38.179	283.175	283.146	$C_{12}H_{26}O_7$	Hexaethylene glycol
19	38.179	467.289	467.276	$C_{19}H_{26}N_6O_8$	(2S)-2-[[2-[[(2S,3S,5R)-3-azido-5-[(5-methyl-2,4-dioxopyrimidin-1-yl)methyl] oxolan-2-yl]methoxy]-2-oxoacetyl]amino]-4-methylpentanoic acid

(to be continued)

Continued Table 1

No.	t_R (min)	Precursor ion $[M + H]^+$ (*m*/*z*)	Theoretical mass (*m*/*z*)	Elemental composition	Name of the compound
20	38.446	277.167	277.165	$C_{14}H_{20}N_4O_2$	P-coumaroylagmatine
21	38.446	122.097	122.085	$C_8H_{11}N$	Phenethylamine
22	39.421	423.092	423.076	$C_{19}H_{18}O_{11}$	Mangiferin
23	39.021	441.102	441.102	$C_{19}H_{20}O_{12}$	3,5-Dihydroxyphenyl 1-O-(6-O-galloyl-beta-D-glucopyranoside)
24	39.021	463.084	463.075	$C_{17}H_{14}N_6O_{10}$	2-(2-Aminoethylamino)-1,3-bis(3,5-dinitrophenyl)propane-1,3-dione
25	39.421	307.176	307.175	$C_{15}H_{22}N_4O_3$	Propentofylline
26	40.572	355.102	355.103	$C_{16}H_{18}O_9$	Chlorogenic acid
27	4.056	136.062	136.062	$C_5H_5N_5$	Adenine
28	4.409	124.040	124.039	$C_6H_5NO_2$	Nicotinic acid
29	36.706	205.096	205.097	$C_{11}H_{12}N_2O_2$	Tryptophan
30	4.056	136.062	136.062	$C_5H_5N_5$	Adenine

Table 2 Compounds identifi ed in SDL extract by LC-MS/MS at negative ion mode

No.	t_R (min)	Precursor ion $[M + H]^-$ (*m*/*z*)	Theoretical mass (*m*/*z*)	Elemental composition	Name of the compound
1	46.696	179.034	179.026	$C_9H_8O_4$	Caffeic acid
2	39.770	233.067	233.132	$C_{10}H_{10}O_4$	Ferulic acid
3	2.169	165.041	165.158	$C_9H_8O_3$	P-coumaric acid

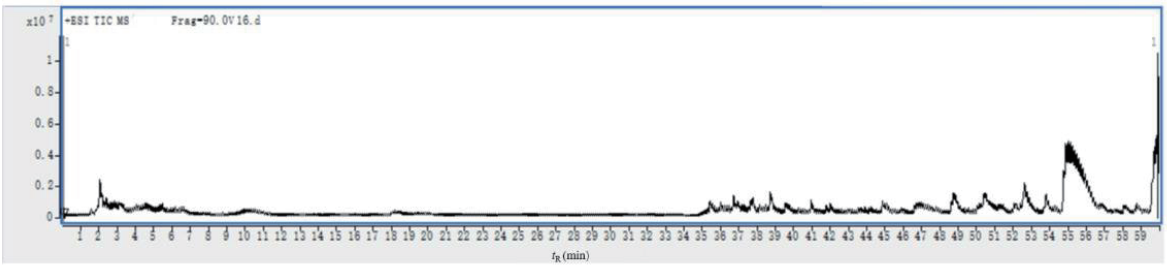

Fig. 1 Total ion chromatogram of positive ion LC-MS/MS of SNL extract

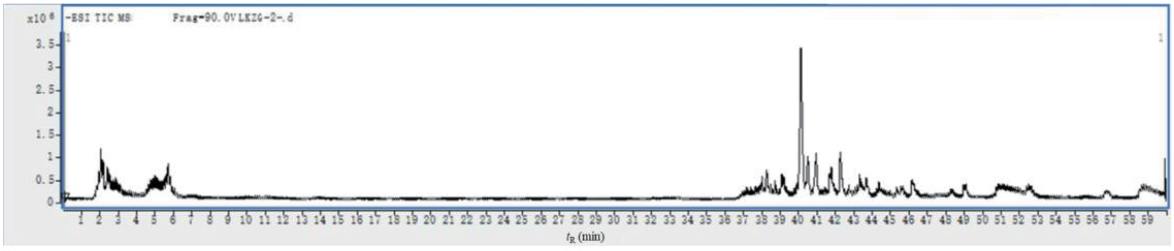

Fig. 2 Total ion chromatogram of negative ion LC-MS/MS of SNL extract

3.3 Active ingredient screening and target prediction

In order to better demonstrate the intricate relationship between active ingredients and targets, Cytoscape 3.9.0 software was used to construct a compound-target network graph, which contained 432 nodes and 431 edges (Fig. 3).

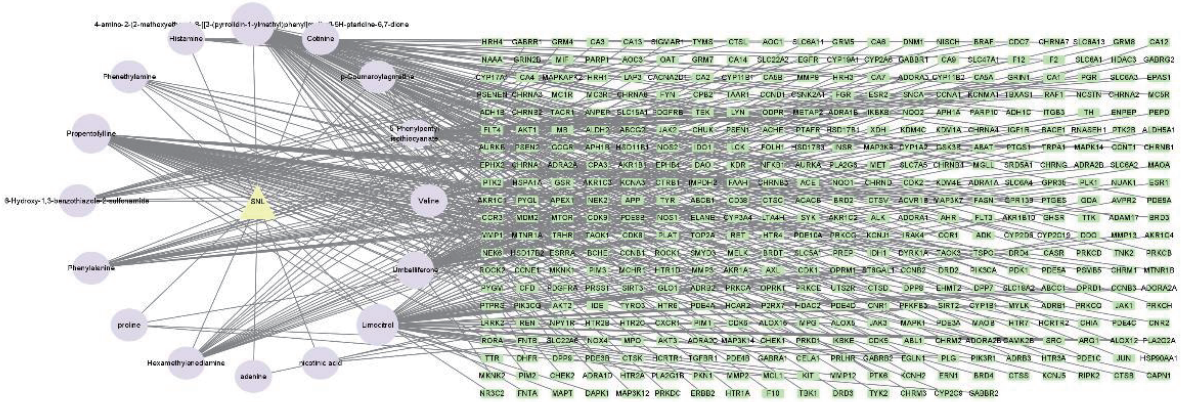

Fig. 3 "Compounds-targets" network

3.4 Disease target prediction results

The target targets were screened by GeneCards and OMIM databases, and a total of 1 981 colitis disease targets were obtained after deleting duplicates. By importing the Venn diagram of Venny 2.1.0 online tool together with 462 active ingredient targets for comparison, 157 core gene targets were obtained (Fig. 4).

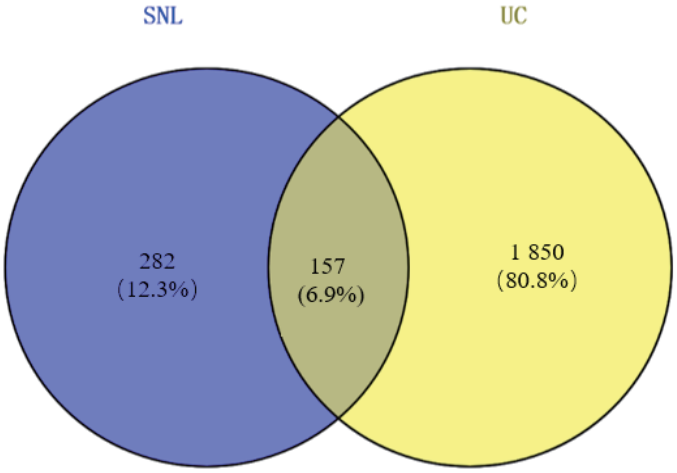

Fig. 4 "Disease-component" target Venn diagram

3.5 Construction of protein interaction network PPI results

The biological species was set as "Homo sapiens", and 157 core gene targets were selected through the Veen. The components and corresponding target information were imported into the String database to draw the interaction network, and the confidence level was selected as 0.400. The obtained core targets were saved and imported into Cytoscape 3.9.0 to draw the protein-protein interaction network of the core proteins. The protein interaction information was obtained with 157 nodes and 1 892 edges (Fig. 5). The higher the number of targets connected to each target, the larger the node area, and the darker the color, the more important the target is in the protein interaction network.

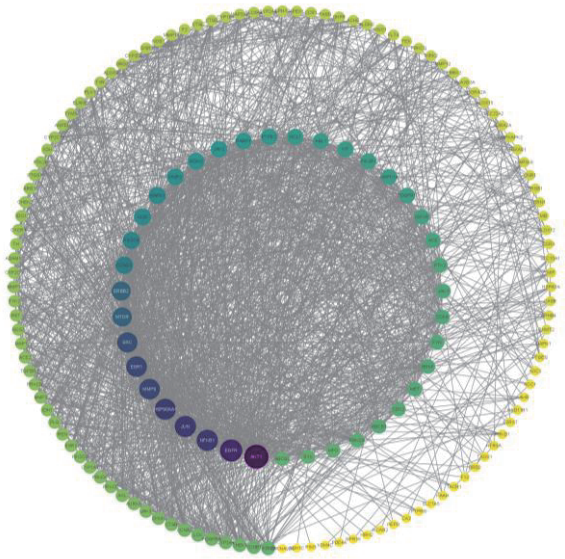

Fig. 5 Network of protein-protein interaction

3.6 Gene function and pathway analysis

In order to investigate the mechanism of action of these key target genes in UC, GO bioprocess analysis and KEGG enrichment analysis were performed using Microbiotics online tools.

3.6.1 GO bioprocess analysis

GO bioprocess analysis involving 557 bioprocesses, phosphorylation, protein phosphorylation, signaling, negative regulation of apoptotic processes, inflammatory response, protein autophosphorylation, intracellular signaling, positive regulation of RNA polymerase Promoter transcription, response to xenobiotic stimuli, positive regulation of cell proliferation, negative regulation of apoptotic processes, positive regulation of apoptotic processes, INNATE immune response, proteolysis, response to xenobiotic stimuli, positive regulation of apoptosis, negative regulation of apoptosis, negative regulation of apoptosis, and positive regulation of apoptotic processes. Promoter transcription, response to xenobiotic stimuli, positive regulation of cell proliferation, apoptotic process, INNATE immune response, proteolysis, positive regulation of protein kinase B signaling, positive regulation of ERK1 and ERK2 cascade, peptidyl-serine phosphorylation, positive regulation of protein kinase B signaling. Serine phosphorylation, positive regulation of cell migration, negative regulation of gene expression, positive regulation of transcription, DNA catalysis, peptidyl-tyrosine phosphorylation; 88 cellular components, cytoplasmic membrane, cytoplasm, nucleus, cytosolic membrane, nucleoplasm, exocytosis, extracellular region, extracellular space, mitochondrion, perinuclear region of the cytoplasm, intracellular membrane bounded organelles, membrane rafts, endoplasmic reticulum membrane, cellular surface, receptor complexes, apical plasma membrane, macromolecular complexes, outer plasma membrane, glutamatergic synapses; 124 molecular function, protein kinase activity, protein tyrosine kinase activity, ATP-binding, protein serine/threonine kinase activity, transmembrane receptor protein tyrosine kinase activity, enzyme-binding, non-transmembrane protein tyrosine kinase activity, kinase activity, homologous protein-binding, as shown in Fig. 6.

3.6.2 KEGG pathway enrichment analysis

The KEGG pathway enrichment analysis is shown in Fig. 7, involving 154 pathways, including pathways in cancer, metabolic pathways, PI3K-Akt signaling pathway, MAPK signaling pathway, hepatitis B, proteoglycans in cancer, Rap1 signaling pathway,

lipids and atherosclerosis, chemocarcinogenesis − reactive oxygen species (ROS), and human cytomegalovirus infection. Reactive oxygen species, cytomegalovirus infection.

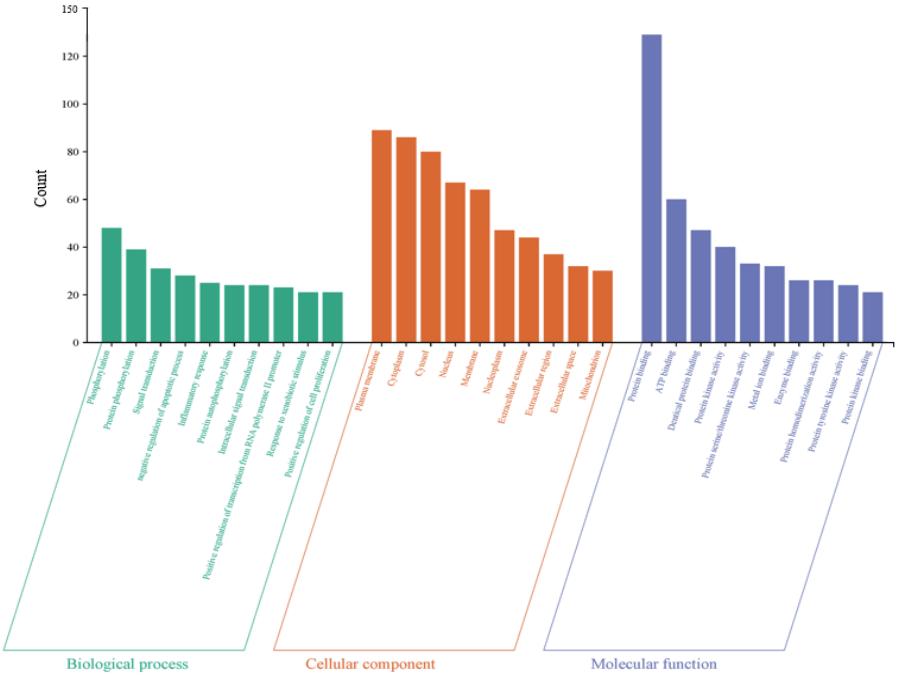

Fig. 6 GO functional enrichment analysis diagram

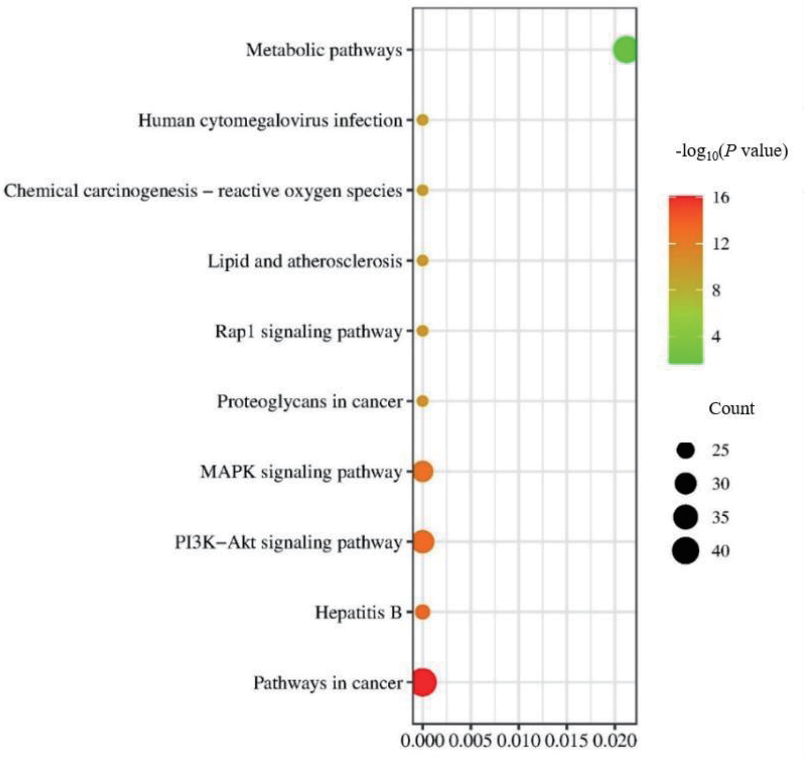

Fig. 7 KEGG Pathway enrichment analysis

3.6.3 Prediction of key active ingredients

The top five of the degree were chosen, as shown in Table 3.

Table 3 Key active ingredients (Degree > 10)

Degree	Name
71	4-amino-2-(2-methoxyethoxy)-8-[[3-(pyrrolidin-1-ylmethyl)phenyl]methyl]-5H-pteridine-6,7-dione
66	Limocitrol
61	Propentofylline
44	Umbelliferone
34	5-Phenylpentyl isothiocyanate

3.7 Molecular docking

In order to further clarify the molecular binding ability between the potential active ingredients and key target proteins for the treatment of UC, based on the results of network pharmacology analysis, the top 5 active ingredients with the highest degree value, 4-amino-2-(2-methoxyethoxy)-8-[[3-(pyrrolidin-1-ylmethyl)phenyl] methyl]-5H-pteridine-6,7-dione, Limocitrol, Propentofylline, Umbelliferone, 5-Phenylpentyl isothiocyanate , degree value of the top 5 core targets AKT1, EGFR, NFKB1, JUN, and HSP90AA1, and the docking results are detailed in Table 4. The docking scores were all greater than 100, indicating that these compounds and proteins could dock well, further proving the reliability and effectiveness of SNL in the treatment of UC. 2D and 3D mapping clearly illustrated the binding patterns of the compound-protein docking results. The 2D and 3D maps (Fig. 8 and Fig. 9) clearly illustrated the binding pattern of the compound-protein docking results, which showed that the potential active ingredients of SNL are strongly related to the key targets of UC, and these ingredients and targets are likely to be the material basis and key targets of SNL for the treatment of UC.

Table 4 Interaction between the active substance and the target protein

Entry	Protein	PDB ID	LibDock score	Interaction
4-amino-2-(2-methoxyethoxy)-8-[[3-(pyrrolidin-1-ylmethyl)phenyl] methyl]-5H-pteridine-6,7-dione	AKT1	6HHG	120.879	Attractive char; Pi-Sigma; Conventional hydrogen; Pi-Alkyl; Carbon hydrogen bond
	EGFR	7U99	121.346	Pi cation; Attractive harge; Conventional hydrogen bond; Amide pi-stackedcarbon hydrogen bond; Pi-alkyl
	NFKB1	5NJX	108.757	Conventional hydrogen bond; Unfavorable acceptor-acceptor; Carbon hydrogen bond; Pi-alky1; Unfavorable donor-donor
Propentofylline	AKT1	6HHG	114.031	Conventional hydrogen bond; Alky1; Carbon hydrogen bond; Pi-alky1; Pi-cation
	JUN	2P33	112.274	Carbon hydrogen bond; Alky1; Unfavorable acceptor-acceptor; Pi-alkyl; Pi-cation
	NFKB1	100A	126.143	Carbon hydrogen bond; Alky1; Unfavorable acceptor-acceptor; Pi-alkyl; Pi-cation

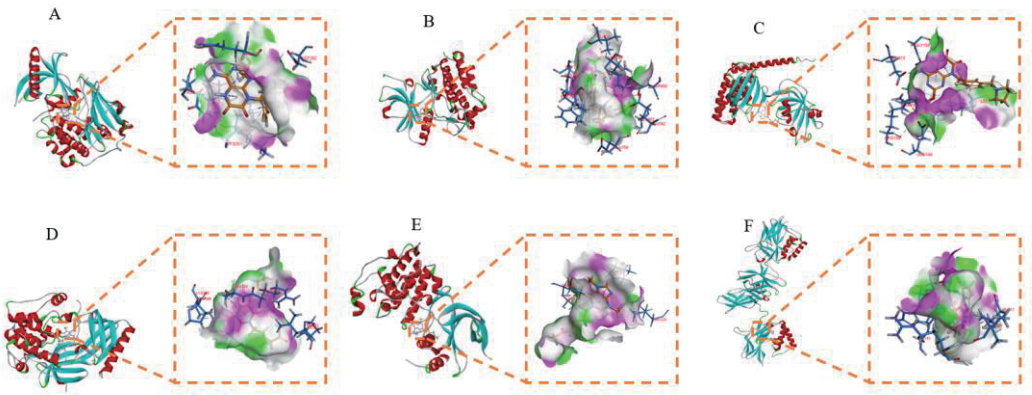

Fig. 8 SNL of molecular docking between key compounds and core target proteins

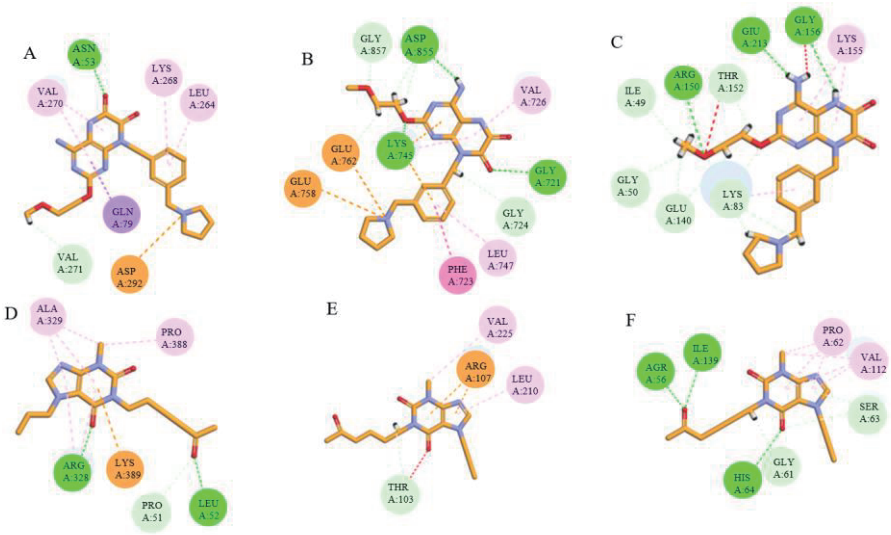

Fig. 9 2D model diagram of the docking between SNL components and target proteins

4 Discussion

With the improvement of living standards, the incidence of UC has been increasing in recent years, and the prolonged and difficult to cure UC has led to a gradual decline in the digestive ability of the patients, intestinal malabsorption, and then malnutrition, immune dysfunction and other complications, which makes the clinical treatment quite tricky [5]. The pathogenesis of UC is complex, and there is no clear conclusion yet, and it may be associated with the interaction of genetic, immune, infectious and mental factors, in which the balance of inflammatory factors plays an important role [6]. The balance of inflammatory factors plays an important role [7], such as the infiltration of inflammatory cells and the abnormal expression of inflammatory mediators [8], the imbalance of anti-inflammatory factors and pro-inflammatory factors, as well as the immune response caused by the imbalance of its balance can lead to an imbalance of the immune function of the colon and disorders, which can lead to damage to the colon mucosa and thus lead to the development of UC, and ultimately lead to chronic inflammation [9].

SNL is a traditional Chinese medicine with dual use of medicine and food, which was recorded in the “Compendium of Materia Medica”, and is widely distributed in Heilongjiang, Hebei, Sichuan,

and Guangdong in China, and mainly produced in South Africa and India in foreign countries. It is rich in nutrients, comprehensive and diversified in pharmacological effects, and has good practical application value [9]. It has been proved to have good activity in antioxidant, anti-inflammatory, intestinal protection, antibacterial, antiviral and antitumor [10]. There are relatively few reports on polyphenolic components in SNL, research has showed that phenolic acids were distributed in all parts of the plant, and the total content, from the largest to the smallest, was in the order of ripe fruits, leaves, green fruits, and stems, which were dominated by chlorogenic acid and caffeic acid [11]. Among them, chlorogenic acid has antibacterial, anti-inflammatory, detoxification, choleretic, antihypertensive and elevation of white blood cells and significantly increase gastrointestinal peristalsis and promote gastric juice secretion and other pharmacological effects [12].

Using LS-MS/MS to analyze the main constituents in the fruits of SNL were analyzed, and a total of 33 substances were derived, which contained 5 phenolic acids: Ferulic acid, caffeic acid, p-coumaric acid, chlorogenic acid, and nicotinic acid. The mechanism of action of SNL in the treatment of UC was explored by using network pharmacology, which suggests that SNL can exert its therapeutic effect in the treatment of UC through multi-components and multi-targets. The results of PPI network interaction analysis suggested that SNL could treat UC by acting on the core targets of AKT1, EGFR, NFKB1, JUN, HSP90AA1, MMP9, etc. Epidermal growth factor (EGFR) is a member of the epidermal receptor family of transmembrane tyrosine kinase receptors [13], which can mediate cellular differentiation, proliferation, growth, and migration, and stimulate the up-regulation of EGFR expression in the event of tissue injury, and EGFR activation can reduce early intestinal inflammation [14]. HSP90AA1 can specifically activate cytotoxic T cells [15], and the expression of HSP90AA1 is positively correlated with the expression of interleukin 6 (IL-6), so that the inhibition of HSP90AA1 can suppress cellular immunity and reduce the secretion of inflammatory factors [16]. Through KEGG enrichment analysis, several important signaling pathways were predicted, which were mainly related to pathways in cancer, metabolic pathways, MAPK signaling pathway, and the abnormal activation of PI3K/AKT pathway in the pathogenesis of UC. Activation of the PI3K/AKT pathway plays an important role in the pathogenesis of UC [17], which can inhibit the secretion of inflammatory factors such as TNF-α and IL-6 by inhibiting the phosphorylation of PI3K and down-regulating the activation of AKT, thus exerting its anti-inflammatory effect [18]. Inhibiting the PI3K/Akt/NF-κB signaling pathway can improve UC [19].

5 Conclusion

To summarize, this experiment identified the active ingredients in SNL through LC-MS/MS, and network pharmacology technology predicted the interaction between the main active ingredients, targets, and pathways of SNL. Molecular docking technology proved the interaction between the main active ingredients and core targets of SNL in treating UC, further confirming the accuracy and reliability of network pharmacology prediction results. It is speculated that SNL may exert therapeutic effects on UC by inhibiting the PI3K/Akt/NF-κB signaling pathway. This study provides a reference for further in-depth research on the mechanism of action of SNL in treating UC.

References

[1] Zhang SH, Shen H, Zheng K, et al. Consensus opinion of traditional chinese medicine diagnosis and treatment experts on ulcerative colitis 2017 [J]. J Tradit Chin Med, 2017, 32 (8): 3585-3589.

[2] Xue YC, Zhou YL, Chen G. Study on the antioxidant activity and anti-fatigue effect of extracts from sunflower fruit [J]. Grain and Oil, 2020, 33 (11): 126-128.

[3] Wang HC, Chung PJ, Wu CH, et al. *Solanum nigrum* L polyphenolic extract inhibits hepatocarcinoma cell growth by inducing G2/M phase arrest and apoptosis [J]. J Sci Food Agric, 2011, 91(1): 178-185.

[4] Shi YB, Geng L, Zhao Y. Optimization of extraction technology by response surface methodology and antioxidant analysis of polyphenols from *Solanum Nigrum* L [J]. Food Industry, 2022, 43 (4): 126-131.

[5] Wu X, Lin L, Qin JJ, et al. CARD3 promotes cerebral is chemia-reperfusion injury via activation of TAK1 [J]. J Am Heart Assoc, 2020 (9): e014920.

[6] Gu SZ, Xue Y, Gao Y, et al. Anti-inflammatory mechanism of Qingdai on ulcerative colitis in intestinal epithelial cell inflammation model [J]. Pharmacol Ther, 2021, 37 (6): 67-71.

[7] Mu N, Liao B, Li Z, et al. Exploring the mechanism of action of Dixiacao in the treatment of ulcerative colitis based on network pharmacology and molecular docking technology [J]. Shandong Science, 2023, 36 (6): 48-55.

[8] Tatiya-Aphiradee N, Chatuphonprasert W, Jarukamjorn K. Immune response and inflammatory pathway of ulcerative colitis [J]. J Basic Clin Physiol Pharmaco, 2018, 30 (1): 1-10.

[9] Zhang T, Huang R. Progress of research on bioactive components of SNL fruit and their pharmacological effects [A]. Health Food R&D and Industrial Technology Innovation Summit Forum and 2022 Annual Conference of Guangdong Food Society [C]. Guangdong: Guangdong Food Society, 2023: 4.

[10] Zhang H, Lv JL, Zheng QS, et al. Active components of Solanum nigrum and their antitumor [J]. Front Oncol, 2023, 19 (3): 13.

[11] Chen JC, Chen W, Wang XJ, et al. Progress on the extraction of chlorogenic acid from the Lebanese medicinal herb SNL oligochaeta [J]. Neijiang Science and Technology, 2023, 44 (3): 114-115.

[12] Hasegawa K, Kuwata K, Yoshitake J, et al. Extracellular vesicles derived from inflamed murine colorectal tissue induce fibroblast proliferation via epidermal growth factor receptor [J]. FEBS J, 2021, 288 (6): 1906-1917.

[13] Meng Y, Wang XH, Liu XL, et al. Determination of polyphenol content in different parts of Lonicera japonica by staining and HPLC [J]. Zhongnan Pharmacology, 2022, 20 (6): 1430-1435.

[14] Sabbah DA, Hajjo R, Sweidan K. Review on epidermal growth factor receptor (EGFR) structure, signaling pathways, interactions, and recent updates of EGFR inhibitors [J]. Curr Top Med Chem, 2020, 20 (10): 815-834.

[15] Liu TH, Liu D, Wang XH, et al. Detection and analysis of HSP60, HSP90 and IL-2, IL-6 in psoriasis lesion tissues [J]. J Dermatol, 2009, 23 (3): 140-141.

[16] Dubé PE, Liu CY, Girish N, et al. Pharmacological activation of epidermal growth factor receptor signaling inhibits colitis-associated cancer in mice[J]. Sci Rep, 2018, 8 (1): 9119.

[17] Zhang M, Peng Y, Yang Z, et al. DAB2IP down-regulates HS Active components of *Solanum nigrum* and their antitumor P90AA1 to inhibit the malignant biological behaviors of colorectal cancer [J]. BMC Cancer, 2022, 22 (1): 561.

[18] Dong L, Du H, Zhang M, et al. Anti-inflammatory effect of Rhein on ulcerative colitis via inhibiting PI3K/Akt/mTOR signaling pathway and regulating gut microbiota [J]. Phytother Res, 2022, 36 (5): 2081-2094.

[19] Li Q, Zheng S, Niu K, et al. Paeoniflorin improves ulcerative colitis via regulation of PI3K-AKT based on network pharmacology analysis [J]. Exp Ther Med, 2024, 27 (4): 125.